

11,05

Temperature investigations of magnetic properties when analyzing the structural phase state of a model nanocomposite with carbidosteel composition

© A.I. Ulyanov, A.A. Chulkina[¶], A.L. Ulyanov

Udmurt Federal Research Center, Ural Branch Russian Academy of Sciences, Izhevsk, Russia

[¶]E-mail: chulkina@udman.ru

Received May 17, 2022

Revised May 17, 2022

Accepted May 22, 2022

The phase composition, magnetic state of the phases and their influence on the formation of the magnetic hysteresis properties of the nanocomposite with the $(\text{Fe}_{0.85}\text{Mn}_{0.10}\text{Ni}_{0.05})_{83}\text{C}_{17}$ composition after mechanosynthesis and subsequent annealing have been studied. It is shown that, although the dependences of the coercive force on the annealing temperature $H_c(T_{\text{ann}})$ of the alloy, measured at room and liquid nitrogen temperatures, are curves with maxima, the formation of H_c is driven by different mechanisms. At room temperature measurements, the maximum H_c value of the composite is obtained when the size of the ferrite phase precipitates approaches to the critical single-domain state, whereas at low temperature maximum H_c value is caused by the change of the cementite structural state upon annealing.

Keywords: Nanocrystalline Fe–C–Mn–Ni alloys, mechanical alloying, heat treatment, X-Ray diffraction, coercive force, magnetic susceptibility, Curie temperature, Mössbauer spectroscopy.

DOI: 10.21883/PSS.2022.10.54246.381

1. Introduction

Alloys based on the Fe–C system are widely used in various industries. The traditional possibilities of creating new more durable materials based on them have already been largely exhausted. At present, the researchers' interest is largely aimed at studying the nanoscale structural-phase states of steels and alloys, which, according to modern concepts, are the basis for increasing their strength characteristics [1,2]. An effective way to obtain the nanostructured state of bulk materials is considered to be an intense plastic deformation that occurs during the process of torsion under high pressure or equal-channel angular pressing [3,4]. The nanostructural state of iron-based alloys is also easily achieved by the method of mechanical alloying (MA) of the initial powders in a ball planetary mill [5,6]. For research purposes, this method is attractive because on the basis of MA-alloys, by doping and subsequent heat treatment, nanocomposites with a given phase composition can be obtained. Structural-phase analysis of nanocomposites is carried out most often by X-ray methods. At the same time, the relationship of the phase composition, structural state and doping of phases with magnetic properties is known, in particular, with saturation magnetization, coercive force, Curie temperature, respectively [7]. The phases of high-alloy steels and alloys, depending on the degree of doping, can be at room temperature in both ferromagnetic and paramagnetic states. In this regard, temperature measurements of the

magnetic characteristics of nanostructured steels and alloys become relevant. The results of magnetic measurements can be used both to confirm the results of X-ray phase analysis and to obtain more complete information about the structural-phase state, in particular, about the doping of the phases of the studied composites [8,9]. In this study, a mechanosynthesized model alloy of the composition of carbidosteel $(\text{Fe}_{0.85}\text{Mn}_{0.10}\text{Ni}_{0.05})_{83}\text{C}_{17}$ was chosen for structural and magnetic research. The choice of manganese as a carbide-forming element is due to the fact that, firstly, it contributes to the strengthening of the solid phase — cementite. Secondly, Mn is also an element that expands the γ -region of carbon alloys and, therefore, along with Ni, will contribute to the formation of a stronger binding phase of the composite — austenite. In addition, Mn doping effectively lowers the Curie temperature T_C of cementite [10]. In this regard, it becomes possible to study the patterns of redistribution of Mn atoms between cementite and austenite in the process of annealing the nanocomposite under study. Also of interest is the formation of magnetic hysteresis properties of a nanocomposite, the H_c of which can be highly dependent on the dispersion of ferromagnetic phases [11]. It is expected that after high-temperature annealing, a nanocomposite will be formed, consisting of a mixture of nickel-doped (and, possibly, manganese) binding phase — austenite and solid phase — manganese-doped cementite.

2. Specimens and methods of study

The model alloy $(\text{Fe}_{0.85}\text{Mn}_{0.10}\text{Ni}_{0.05})_{83}\text{C}_{17}$ was obtained by the MA method of a mixture of carbonyl iron powders of the OSCh grade 13-2 with a purity of 99.98%, nickel and manganese with a purity of 99.9%, graphite with a purity of 99.99% in a ball planetary mill Pulverisette-7 for 16 h in an argon atmosphere. Average particle size of powder alloys $\sim 5 \mu\text{m}$. The grinding vessels of the mill and balls with a diameter of 8 mm were made of steel ShKh15. The samples were annealed in an argon atmosphere on the setup for measuring the temperature dependence of differential magnetic susceptibility. The rate of heating and cooling of the samples after annealing was 30 deg/min.

X-ray studies were performed at room temperature on a Miniflex 600 diffractometer in Bragg–Brentano geometry in $\text{CoK}\alpha$ -radiation. To decipher the phase composition and determine the size of coherent scattering blocks, a software package for full-profile analysis of diffractograms [12] was used. Mössbauer spectra were obtained on the SM2201DR spectrometer in constant acceleration mode with a source of γ -radiation $^{57}\text{Co}(\text{Rh})$. A generalized regularized algorithm [13] was used to reconstruct the distribution function of hyperfine fields $P(H)$ from the spectra. The specific saturation magnetization and coercive force were measured on a vibrating magnetometer with a maximum magnetizing field of 13 kA/cm.

Magnetic and Mössbauer measurements were carried out both at room temperature and at low temperatures, up to the temperature of liquid nitrogen (-196°C).

3. Results and discussion

The phase composition of the model alloy $(\text{Fe}_{0.85}\text{Mn}_{0.10}\text{Ni}_{0.05})_{83}\text{C}_{17}$ after MA and subsequent annealing is given in Table 1.

It can be seen that after MA, the alloys contain mainly an amorphous phase and cementite, as well as a small amount ($\sim 10 \text{ vol.}\%$) of χ -carbide and ferrite. In the process of annealing up to 500°C the transformation of the amorphous phase and χ -carbide into cementite and ferrite occurs, the formation of austenite begins (Table 1). Phase changes are reflected in the magnetic characteristics of the samples (Fig. 1). From the curve 1 in Fig. 1, *a* it can be seen that the specific magnetization of the saturation σ_s of the alloy changes slightly. At the same time, in the interval T_{ann} from 300 to 500°C its coercive force H_c increases intensively (by order of magnitude) (Fig. 1, *b*, curve 1). To understand the high values of H_c of the alloy after annealing at 500°C , information about the magnetic state of its phases is needed, which can be given by Mössbauer studies. Figure 2, *a* shows the Mössbauer spectra of the alloy measured at room temperature.

Mathematical processing of spectra, carried out in a discrete representation, makes it possible to determine the fraction of iron atoms in the phases and the magnetic state

Table 1. X-ray phase constitution of the composite $(\text{Fe}_{0.85}\text{Mn}_{0.10}\text{Ni}_{0.05})_{83}\text{C}_{17}$

$T_{\text{ann}}, ^\circ\text{C}$	Phases, vol.%				
	Amorphous phase	Cementite	Ferrite	χ -carbide	Austenite
After MA	44.4	34.1	11.5	10.0	–
200	29.9	43.6	17.0	9.5	0
300	25.3	48.2	22.5	3.7	0.3
400	20.4	51.5	25.6	1.4	1.1
500	0	66.5	30.1	0	3.4
600	–	65.0	13.0	–	22.0
700	–	64.7	1.8	–	33.5
800	–	59.0	0	–	41.0

of the phases. From Fig. 2, *a* and Table 2 it follows that after annealing at 500°C there are two main phases in the composite: ferrite (component 1) and paramagnetic cementite (component 3), which contain 41 and 55% from all Fe atoms of the alloy, respectively.

The sample also contains a small number ($\sim 4\%$) of Fe atoms of the weakly magnetic phase (component 4). Based on the quantitative ratios of Table 1, such a phase is, most likely, doped austenite. Thus, after annealing at 500°C alloy is basically a composite in which ferrite secretions (particles) are surrounded by paramagnetic cementite. The coercive force of ferrite usually does not exceed 5–10 A/cm [7]. But in this case, it can be assumed that ferrite particles, isolated magnetically, have an average size close to the critical size of the single domain d_{cr} .

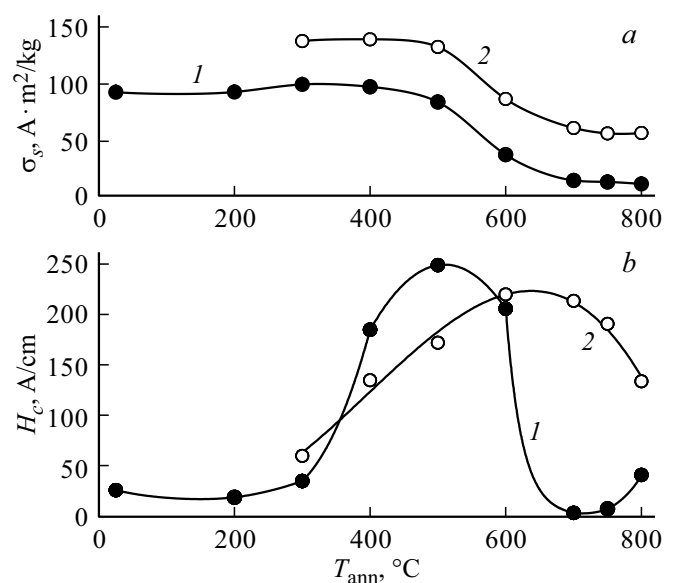


Figure 1. Dependence on the annealing temperature of *a* — specific saturation magnetization σ_s , *b* — coercive force H_c of the composite. Measuring temperature: 1 — room, 2 — (-196°C) .

Table 2. Results of analysis of Mössbauer composite spectra $(\text{Fe}_{0.85}\text{Mn}_{0.10}\text{Ni}_{0.05})_{83}\text{C}_{17}$

$T_{\text{ann}}, ^\circ\text{C}$	Paramagnetic phases, at.% Fe		Ferromagnetic phases, at.% Fe	
	Austenite	Cementite	Ferrite	Cementite/austenite
Measurements at room temperature				
500	0	55	41	–/4
700	29	68	0	3/–
800	36	61	–	3/–
Measurements at $T = -196^\circ\text{C}$				
500	0	–	37	63
700	32	–	0	68/–
800	41	–	–	59/–

It is known [11,14,15] that in the process of measuring H_c the remagnetization of single-domain iron particles occurs by irreversible rotation of magnetization, which provides high (500 A/cm and higher) values of their H_c . For iron particles, $d_{\text{cr}} \approx 14\text{--}18$ nm. The predominantly Ni-doped Fe particles most likely have higher values of d_{cr} , since for nickel particles $d_{\text{cr}} \approx 72$ nm [14].

The annealed samples were determined to have an average size of coherent scattering regions $\langle D \rangle$, which with high probability determine the average size of phase secretions. For example, the ferrite in the sample annealed by $T_{\text{ann}} = 500^\circ\text{C}$ has $\langle D \rangle \approx 60$ nm. Taking into account this data, it can be concluded that the critical size of the single domain d_{cr} of particles of predominantly Ni-doped ferrite is near ~ 60 nm. Thus, the increase in the values of H_c of the composite up to 250 A/cm in the annealing temperature range from 300 to 500°C is most likely due to the approximation of the average size of ferrite secretions surrounded by paramagnetic cementite to the critical size of their single domain. The proposed mechanism of remagnetization also explains the decrease in H_c of the composite in the range of T_{ann} from 500 to 700°C , within which the content of the ferritic phase decreases intensively from ~ 30 vol.% and, practically, to zero values (Table 1). As a result, H_c of the composite drops sharply to the value of ~ 3 A/cm (Fig. 1, *b*, curve *I*), due to the presence, as will be shown below, the weakly magnetic cementite with T_C near the room temperature. The Mössbauer spectrum of a sample annealed at 700°C is not given in Fig. 2, as it is in many ways similar to the spectrum of the sample after annealing at 800°C .

A decrease in the content of the ferritic phase in the range T_{ann} from 500 to 700°C (Table 1), as well as an increase in the amount of paramagnetic austenitic phase (Tables 1, 2) cause a decrease in σ_s composite (Fig. 1, *a*, curve *I*).

The paramagnetic state of the cementite of alloy at room temperature means that its T_C is in the region of negative temperatures. In this regard, there is a need for information about the magnetic state of the phases at low measurement temperatures. To this end, at the $T = (-196^\circ\text{C})$, the

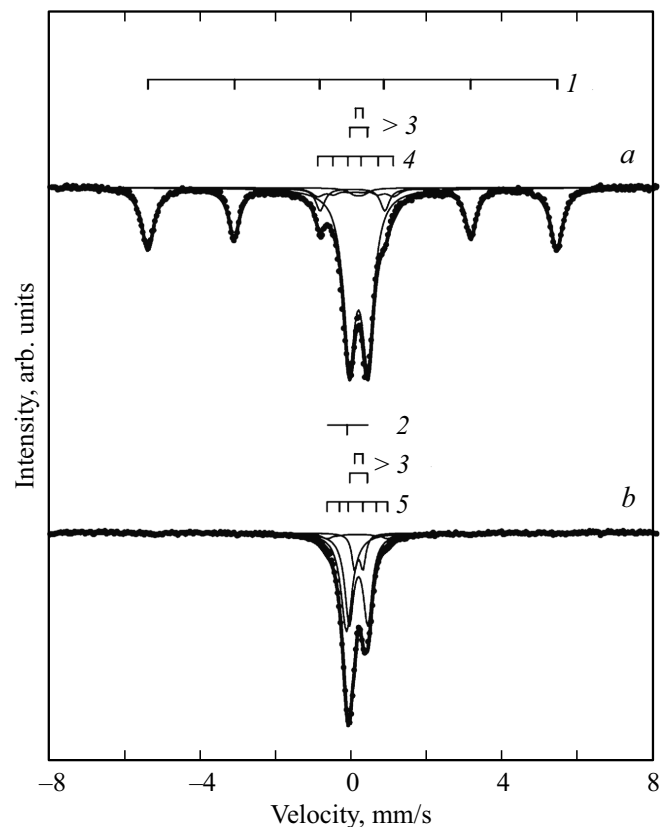


Figure 2. Mössbauer spectra of a composite after annealing at temperatures: *a* — 500°C ; *b* — 800°C . Components of discrete decomposition: *1* — ferrite, *2* — paramagnetic austenite, *3* — paramagnetic cementite; *4* — weakly magnetic austenite, *5* — weakly magnetic cementite. The measurement temperature is room temperature.

Mössbauer spectra of alloy samples annealed at 500, 700 and 800°C were taken. Figure 3 shows (with the exception of the sample with $T_{\text{ann}} = 700^\circ\text{C}$) spectra and components of discrete processing of the spectra of the samples under study. On the right are also the results of processing spectra in a continuous representation in the form of the

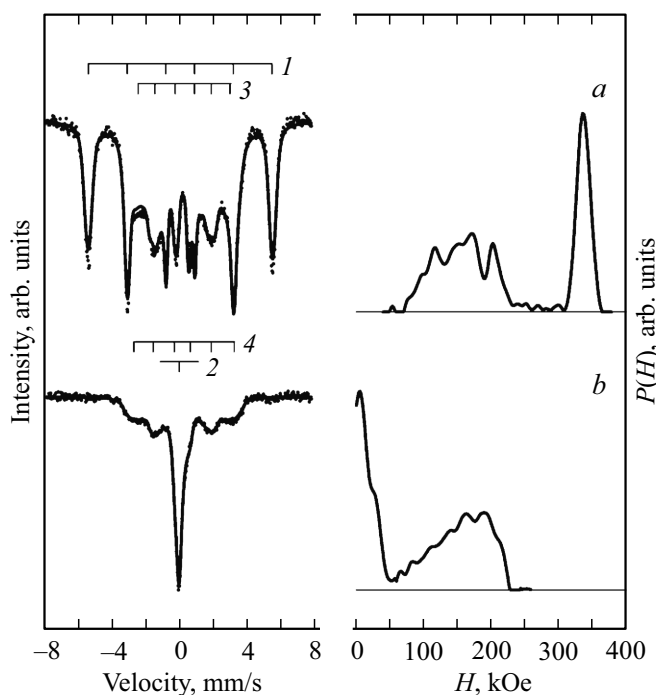


Figure 3. Mössbauer spectra and functions $P(H)$ of the studied composite after annealing at temperatures: a — 500; b — 800°C. Components of discrete decomposition: 1 — ferrite, 2 — paramagnetic austenite, 3 — ferromagnetic cementite and austenite (mixture); 4 — ferromagnetic cementite. Spectra are measured at $T = (-196)^\circ\text{C}$.

function $P(H)$, which reflects the distribution of hyperfine magnetic fields H on the nuclei of the Fe isotopes from the atoms of the immediate environment. Thus, for ferrite, the function $P(H)$ is a pronounced peak with a maximum in the field $H = 337$ kOe (Fig. 3, a). For mainly Mn-doped cementite, the function $P(H)$ lies in the field range ~ 60 –230 kOe (Fig. 3, a and b). For paramagnetic austenite, the maximum function $P(H)$ is near the field $H \approx 0$ kOe (Fig. 3, b). From Fig. 3, a and Table 2 it follows that the ferrite and cementite of the annealed at 500°C alloy, at T measurements -196°C are in a ferromagnetic state (components 1 and 3 in Fig. 3, a). Ferrite contains 37% of the total number of Fe alloy atoms. The rest of the iron (63 at.%) is in cementite and in a small amount (3.4 vol.%, Table 1) of ferromagnetic austenite. The presence of ferromagnetic austenite in the alloy is evidenced by the wide distribution of the function $P(H)$ in the range H from ~ 50 to 300 kOe, which cannot be separated with the distribution of the function $P(H)$ of ferromagnetic cementite. Thus, at a measurement temperature of $T = -196^\circ\text{C}$, the composite after annealing at 500°C magnetically represents ferritic phase secretions located in a matrix of hard-magnetic cementite. The coercive force of ferrite secretions in this situation cannot be higher than H_c of cementite, even if they are in a single domain state after magnetization.

After annealing at 700–800°C the composite consists of a mixture of phases — ferromagnetic cementite and

paramagnetic austenite (components $2, 4$ in Fig. 3, b , Table 2). Since at the temperature of liquid nitrogen cementite after annealing is in a ferromagnetic state, the dependence of $H_c(T_{\text{ann}})$ of the composite (Fig. 1, b , curve 2) in the entire range T_{ann} is determined by the structural state of the cementite [9,16] and the amount of ferritic phase. The higher values σ_s of dependence $\sigma_s(T_{\text{ann}})$ measured at the temperature of liquid nitrogen (Fig. 1, a) are mainly due to the transition of cementite from the paramagnetic to the ferromagnetic state.

The transition of phases, in particular cementite, from the paramagnetic to the ferromagnetic state when the measurement temperature T decreases allows one to determine T_C of the cementite by the magnetic method. Information on the T_C of cementite opens up the possibility of studying the redistribution of Mn between the phases of the composite during annealing.

Several magnetic methods are known for determining T_C of ferromagnetic phases [9,17,18]. In this study, the method of temperature dependence of the magnetic susceptibility of $\chi(T)$ samples was used to find T_C of ferromagnetic cementite in the region of positive measurement temperatures T . In this case, T_C of phases was determined by the temperature of the maxima of the curves $\chi(T)$. The dependencies of $\chi(T)$ were measured during cooling of alloy samples to room temperature after annealing in the range $T_{\text{ann}} = 300$ –800°C. It was found that after annealing at $T_{\text{ann}} < 700^\circ\text{C}$ maxima on the cooling curves $\chi(T)$ of the samples are not observed. Consequently, the T_C of cementite of such samples is in the region below room temperature T_{room} . For example, the curve 1 in Fig. 4 represents the dependence $\chi/\chi_{20}(T)$, which was removed when cooling the sample after annealing at 500°C. The horizontal portion of the curve 1 reflects the presence

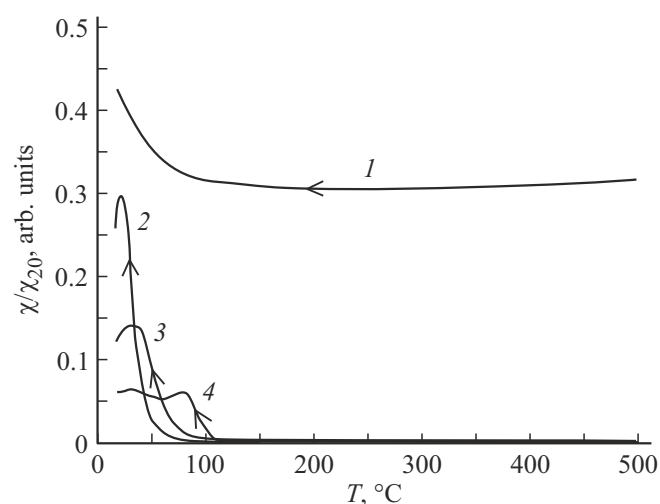


Figure 4. Dependencies of relative magnetic susceptibility χ/χ_{20} on temperature measurements taken when cooling samples of the studied composite after annealing at temperatures: 1 — 500, 2 — 700, 3 — 750, 4 — 800°C. Here χ_{20} — magnetic susceptibility measured at 20°C.

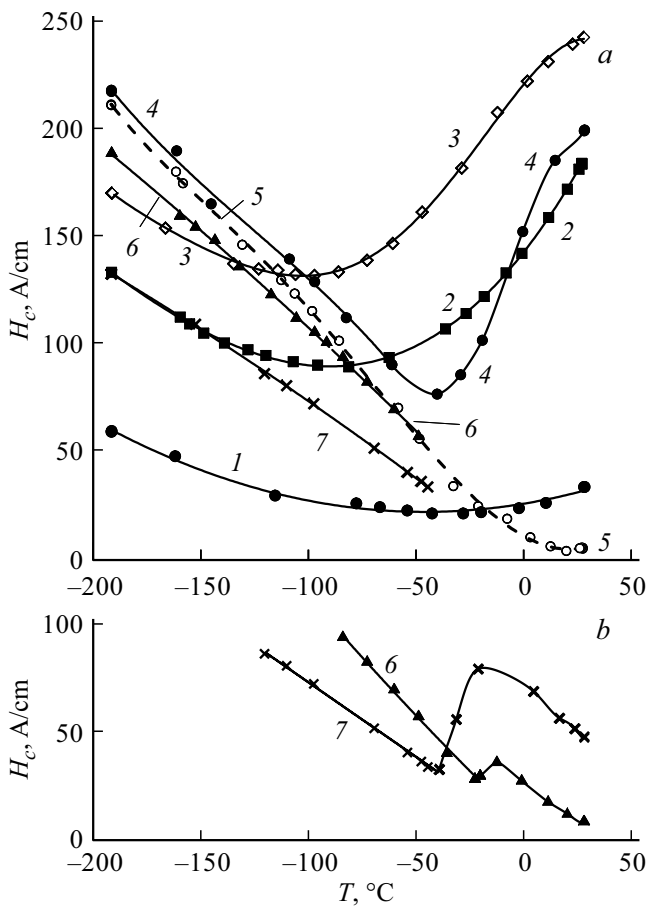


Figure 5. Temperature dependences of the coercive force H_c of the composite, taken after annealing of samples at temperatures: a) 1 — 300, 2 — 400, 3 — 500, 4 — 600, 5 — 700, 6 — 750, 7 — 800°C; b) 6 — 750, 7 — 800°C.

in the sample of the strong magnetic ferritic phase with $T_C > 500^\circ\text{C}$. Gentle rise of the curve 1 indicates, firstly, the approximation of the measurement temperature to T_C of cementite, which is in the region below T_{room} , and secondly, the heterogeneous doping of cementite Mn.

To determine the T_C of Mn-doped cementite, which is located in the measurement temperature region below T_{room} , the method of temperature dependence of the coercive force $H_c(T)$ of the samples was used. Fig. 5 shows the dependences of $H_c(T)$ taken during cooling of annealed composite samples from T_{room} to T of liquid nitrogen (due to the heavy workload of Fig. 5, a with curves, sections of curves 6 and 7 are moved to Fig. 5, b). It can be seen that on the curves $H_c(T)$ there are minimums whose temperature at [9] is close to T_C of cementite. After annealing at 300°C Curie temperature of heterogeneously doped cementite with a strongly distorted crystal lattice is determined by a weakly pronounced and temperature-blurred minimum of the curve $H_c(T)$ in the region of $T \approx -40^\circ\text{C}$ (Fig. 5, a, curve 1). After removal of crystal lattice distortions as a result of annealing at $T_{\text{ann}} > 300^\circ\text{C}$ and increasing the uniformity of doping phases, especially

cementite, the minima on the curves $H_c(T)$ become more vividly expressed (curves 2–7 on Fig. 5).

Figure 6 shows the dependencies of $T_C(T_{\text{ann}})$ of cementite, the analysis of which allows us to judge trends in the redistribution of alloying elements, in particular Mn, between the phases of the alloy. The curve 1 reflects the change in T_C from T_{ann} of „primary“ cementite, i.e. cementite, which was formed during MA and crystallization of the amorphous phase during annealing. The decrease of T_C cementite in the range T_{ann} from 300 to 500°C (curves 1–3, Fig. 5, a) can be explained by additional by doping it with Mn atoms, which are being after MA in large quantities in the segregation along the intergrain boundaries of [19], as well as the possible departure of Ni atoms from cementite.

Annealing in the range from 500 to 700°C (curves 4–5, Fig. 5, a) already lead to an increase in T_C of „primary“ cementite (curve 1 on Fig. 6), which indicates a decrease in its composition of the manganese content. In all probability, during annealing, some of the Mn atoms go from the cementite to form nickel-manganese austenite. This assumption is confirmed by comparing the data of X-ray and Mössbauer measurements. In composite samples annealed in this interval T_{ann} , the volume content of cementite is approximately the same (Table 1). However, as follows from the Mössbauer data measured at T_{room} , after annealing at 500°C, there is 55% in cementite, and after annealing at 700°C — already 71% of all Fe atoms contained in the composite (Table 2), that is, the content of Mn atoms in the cementite lattice after annealing at 700°C becomes less indeed. After annealing at 700°C the Mn-doping of cementite becomes so low that the minimum of the curve 5 in Fig. 5, a already lies in the region of $T > 0^\circ\text{C}$. The value T_C of the cementite of this sample, located near room temperature, was found by measuring the dependence $\chi(T)$ (Fig. 4, curve 2). In addition, it follows from the Mössbauer data that at T_{room} the bulk of the cementite of the alloy annealed at 700°C, which contains 68% of all Fe atoms in the composition of the composite, is paramagnetic. And only a small part of cementite, in which there is 3% of all Fe atoms, is a weakly magnetic ferromagnet, which forms at T_{room} the magnetic properties of this sample.

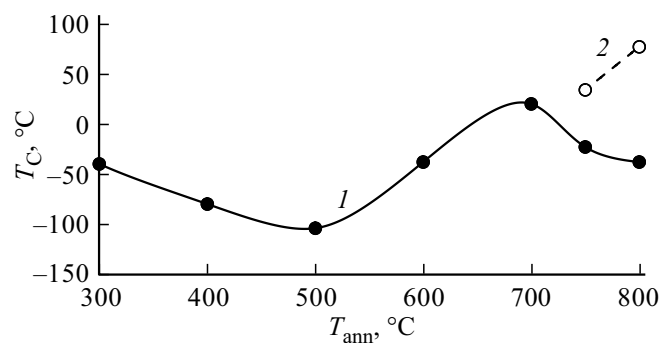


Figure 6. The dependence of the Curie temperature T_C of „primary“ (curve 1) and „secondary“ (curve 2) cementite on the annealing temperature of the studied composite.

After annealing at 750 and 800°C the composite consists of two phases: austenite, paramagnetic even at $T = -196^\circ\text{C}$, and cementite, the magnetic state of which depends on the measurement temperature (Tables 1, 2). It follows from the foregoing that the temperatures of the minima ($T \approx -20^\circ\text{C}$ and $T \approx -40^\circ\text{C}$) on the dependencies $H_c(T)$ (curves 6 and 7 in Fig. 5, *b*), and also of the maxima on the dependencies $\chi(T)$ (curves 2–4 in Fig. 4) characterize the Curie temperature of cementite, but this cementite differs from each other. In the region of negative temperatures are T_C of „primary“ cementite, and in the region of positive temperatures — T_C of cementite, which within the framework of this article we will call „secondary“.

It is known [20] that in the process of high-temperature (over 700°C) annealing, some part of the cementite of alloys dissolves in austenite. Moreover, first of all, areas of undoped, and then weakly-doped cementite are dissolved. The concentration of Mn in the remaining volume of „primary“ cementite becomes higher, which naturally lowers it T_C (Fig. 6, curve 1). When cooled, excess cementite („secondary“) is secreted from austenite, the content of Mn in which is lower, and T_C — higher than that of „primary“ cementite. In this regard, it is logical to assume that the maxima on the dependencies $\chi/\chi_{20}(T)$ of composite $(\text{Fe}_{0.85}\text{Mn}_{0.10}\text{Ni}_{0.05})_{83}\text{C}_{17}$, annealed at 750 and 800°C (curves 3, 4 in Fig. 4) reflect the appearance of „secondary“ cementite with $T_C \approx 34$ and 77°C , respectively (Fig. 6, curve 2). The appearance of „secondary“ cementite, the content of manganese in which decreases with increasing T_{ann} , is, according to [6], the main reason for the increase in H_c of composites after annealing at $T_{\text{ann}} > 700^\circ\text{C}$ (curve 1 in Fig. 1, *b*). Thus, after high-temperature annealing in the alloy, areas of cementite with different Curie temperature values, that is, with different manganese content, are formed.

Annealing at a maximum (for this work) temperature of 800°C completes the main phase transformations characteristic of the solid state of the alloy under study (Tables 1, 2). After such annealing, the alloy is a nanocomposite consisting of the binding phase — of Ni- and Mn-doped paramagnetic austenite, in which the secretions of the strengthening phase — of mainly Mn-doped paramagnetic cementite and a small amount of weakly-doped cementite are placed. The size of secretions of both phases, according to X-ray studies, does not exceed 60 nm.

4. Conclusions

1. The phase composition and formation of the magnetic characteristics of the composite $(\text{Fe}_{0.85}\text{Mn}_{0.10}\text{Ni}_{0.05})_{83}\text{C}_{17}$ after mechanosynthesis and subsequent annealings were studied. It is shown that after annealing at 500°C, the composite is a matrix of paramagnetic cementite, in which there are ferritic phase secretions close to the critical

size of the single domain, which ensures a high value of its $H_c \approx 250 \text{ A/cm}$.

2. The dependence of $H_c(T_{\text{ann}})$, measured at the temperature of liquid nitrogen, is also a curve with a maximum at 600°C, which is due to another mechanism — change in the structural state of cementite during annealing.

3. It is shown that at $T_{\text{ann}} \geq 500^\circ\text{C}$ the segregation of Mn atoms from cementite occurs. It has been suggested that manganese segregated from cementite is used to form nickel-manganese austenite.

4. Annealings at temperatures above 700°C lead to the dissolution of the low-alloyed part of the cementite in austenite and the secretion of manganese-depleted „secondary“ cementite from it in the process of subsequent cooling. As a result, after high-temperature annealing, cementite with different Curie temperature values and therefore with different contents of Mn is observed in composites.

5. After annealing at 800°C alloy $(\text{Fe}_{0.85}\text{Mn}_{0.10}\text{Ni}_{0.05})_{83}\text{C}_{17}$ is a nanocomposite consisting of a binding phase — of austenite, in which nanoscale secretions of the solid phase cementite are placed.

Funding

The work was carried out as part of the state task of the Ministry of Education and Science of the Russian Federation (project No. BB_2021_121030100003-7) using the equipment of the Center for Collective Usage „Center for Physical and Physico-Chemical Methods of Analysis, Research of Properties and Characteristics of the Surface, Nanostructures, Materials and Products“ UdmFITS UB RAS, supported by the Ministry of Education and Science of the Russian Federation within the framework of the Federal Target Program (unique project identifier — RFMEFI62119X0035).

Conflict of interest

The authors declare that they have no conflict of interest.

References

- [1] A.I. Gusev. Nanomaterialy, nanostruktury, nanotekhnologii. Fizmatlit, M. (2009). 416 p. (in Russian).
- [2] N.A. Koneva, E.V. Kozlov, A.N. Zhdanov. Bulletin of the Russian Academy of Sciences: Physics. **70**, *4*, 663 (2006).
- [3] Yu. Ivanisenko, W. Lojkowski, R.Z. Valiev, H.-J. Fecht. Acta Materialia **51**, *18*, 5555 (2003).
- [4] R.Z. Valiev, I.V. Alexandrov. Ob'yomnye nanokristallicheskie materialy: poluchenie, struktura i svoistva. Akademkniga, M. (2007). 398 p. (in Russian).
- [5] Y.Z. Chen, A. Herz, Y.J. Li, C. Borchers, P. Choi, D. Raabe, R. Kirchheim. Acta Materialia **61**, *9*, 3172 (2013).
- [6] Z.G. Liu, X.J. Hao, K. Masuyama, K. Tsuchiya, M. Umamoto, S.M. Hao. Scripta Materialia **44**, *8*, 1775 (2001).

- [7] M.N. Mikheev, E.S. Gorkunov. Magnitnye metody strukturnogo analiza i nerazrushayushchego kontrolya. Nauka, M. (1993). 252 p. (in Russian).
- [8] F.G. Caballero, M.K. Miller, C. Garcia-Mateo, C. Capdevila, S.S. Babu. *Acta Materialia* **56**, 2, 188 (2008).
- [9] A.I. Ulyanov, A.A. Chulkina, V.A. Volkov, E.P. Elsukov, A.V. Zagainov, A.V. Protasov, I.A. Zykina. *The Physics of Metals and Metallography* **113**, 12, 1134 (2012).
- [10] E. Bruck. In: *Handbook of Magnetic Materials* / Ed. K.H.J. Buschow. **17**, Ch. 4. Elsevier, Amsterdam, North Holland (2008). P. 235.
- [11] S.V. Vonsovsky. *Magnetizm*. Nauka, M. (1971). 1032 p. (in Russian).
- [12] N.P. Dyakonova, E.V. Shelekhov, T.A. Sviridova, A.A. Reznikov. *Zavod. lab.* **63**, 10, 17 (1997) (in Russian).
- [13] E.V. Voronina, N.V. Ershov, A.L. Ageev, Yu.A. Babanov. *Phys. Status Solidi B* **160**, 2, 625 (1990).
- [14] V.I. Petinov. *Technical Physics* **59**, 1, 6 (2014).
- [15] G.I. Frolov, O.I. Bachina, M.M. Zavyalova, S.I. Ravochkin. *Technical Physics* **53**, 8, 1059 (2008).
- [16] A.K. Arzhnikov, L.V. Dobyshcheva, C. Demangeat. *J. Phys.: Condens. Matter* **19**, 19, 196214 (2007).
- [17] B.A. Apaev. *Fazovyi magnitnyi analiz splavov*. Metallurgiya, M. (1976). 280 p. (in Russian).
- [18] S. Tikazumi. *Fizika ferromagnetizma. Magnitniye svoistva veshchestva*. Mir, M. (1983). 304 p. (in Russian).
- [19] E.P. Elsukov, G.A. Dorofeev, V.V. Boldyrev. *Doklady Chemistry* **391**, 4–6, 206 (2003).
- [20] M.I. Goldstein, S.V. Grachev, Yu.G. Veksler. *Spetsialniye stali*. MISIS, M., (1999). 408 p. (in Russian).